Available online at www.sciencedirect.com
ScienceDirect
Journal of Bionic Engineering 14 (2017) 520–531

Influence of PVD-duplex-treated, Bionic Surface Structures on the Wetting Behavior for Sheet-Bulk Metal Forming Tools

Wolfgang Tillmann, Dominic Stangier, Nelson Filipe Lopes Dias

Institute of Materials Engineering, *TU Dortmund*, 44227 *Dortmund*, *Germany*,
Leonhard-Euler-Straße 2

Abstract

Bionic surface structures, inspired by the flora, were developed for Sheet-Bulk Metal Forming (SBMF) in order to locally control the friction condition by adjusting the wetting behavior. Five bionic structures were micromilled on ASP®2023 in annealed as well as hardened and tempered conditions. Subsequently, the structured surfaces were plasma-nitrided and coated with a CrAlN thin film. The influence of the treatment method on the structural geometry was investigated with the aid of a scanning electron microscope and 3D-profilometer. The wetting behaviors of water and deep drawing oil (Berufluid ST6007) on bionic surfaces were evaluated using contact angle measurements. The resulting micro-milled structures exhibit an almost identical shape as their bionic models. However, the roughness of the structured surfaces is influenced by the microstructure. The combination of plasma-nitriding and Physical Vapor Deposition (PVD) leads to an increase in roughness. All bionic structures possess higher contact angles than that of the unstructured surfaces when wetted by water. This can be explained by the fact that the structural elevations block the spreading. When the bionic surfaces are wetted by deep drawing oil, the lubricant spreads in the structural cavities, leading to smaller contact angles. Furthermore, the anisotropy of the structure has an influence on the wetting behavior.

Keywords: bionic structures, sheet-bulk metal forming, CrAlN, PVD-duplex treatment, wetting behavior

doi: 10.1016/S1672-6529(16)60418-3

1 Introduction

Sheet-Bulk Metal Forming (SBMF) is a manufacturing technology to produce complex high-strength sheet metal components with the thicknesses of up to 3 mm, with local functional features[1]. SBMF is characterized by the application of a three-dimensional stress, which is similar to bulk forming processes, in order to form locally shaped elements on a sheet metal[2]. However, forming high-strength materials imposes high demands on the forming process. On the one hand, a high strength causes high tribological loads in the contact zone. On the other hand, the formability of the sheet metal decreases when increasing the material strength[3]. A modification of the tool surface enables to sustain high tribological loads and, at the same time, to adjust the material flow[4].

An appropriate method to increase the wear resistance of forming tools is the duplex treatment, which combines a thermochemical plasma-nitriding process with a subsequent deposition of a PVD coating[5]. The plasma-nitriding treatment does not only increase the hardness of the subsurface zone, but also further enhance the tribological performance of the coating. Applying a wear resistant PVD coating onto the surface of the tool reduces the tool's wear and extends the tool life[6]. Ceramic hard thin films have the best properties for the use in the forming technology[7]. Due to the properties of Cr-based nitridic coatings such as a high hardness and lower Young's modulus compared to Ti-based coatings, a low adhesion to counterparts, as well as a low coefficient of static friction, these coatings are especially suitable for forming tools[7].

In order to form components with local functional features, it is necessary to control the material flow by-locally adjusting the friction[8]. A geometric modification of the surface changes the contact condition between the tool and the workpiece and thereby adjusts the

Corresponding author: Dominic Stangier
E-mail: dominic.stangier@tu-dortmund.de

friction behavior. Besides conventional technical surface structures, bionic structures that are inspired by flora and fauna, are particularly promising as their structural patterns are adapted to changing conditions in nature. Bionic structures with concave, convex, and wave-like textures have already been developed for SBMF processes. The structures were based on the surfaces of the shell of beetles living in abrasive, erosive, and adhesive environments[9–11]. Combining bionic structures with CrAlN thin layers reduced the process forces of incremental SBMF by 20% and increased the service life of the tool's surfaces[11].

Another objective of structuring tool surfaces is to locally adjust the wetting behavior with lubricants and thereby to influence the friction behavior. Within this context, hydrophobic plants such as bamboo serve as an inspiration for the development of new bionic structures as reported by Guan *et al*.[12]. Their self-cleaning property results from the hierarchical double structure of their leaves, which leads to a low surface energy[13]. As SBMF operations occur in lubricated condition, it is important to understand the influence of surface modifications on the surface energy as well as the wetting behavior when using forming lubricants. Especially in this context, the approach to modify the contact angle and thus changing the friction conditions under lubrication is promising. Nevertheless, investigations on the wetting behavior of structured forming tool surfaces have not been conducted yet. This paper investigates the bionic structures developed based on the surface of hydrophobic plants. The structures were duplex-treated in order to investigate the interaction between the surface structure and the sequence of treatments, as well as the influence of the coating process on the wettability.

2 Materials and methods

2.1 The development of bionic structures

Five different plants inspired the development of the surface structures for the presented work: The bamboo plants Sasapalmata and Phyllostachys, Chusqueaspectabilis, the spurge Euphorbia myrsinites, as well as the rice plant Oryza sativa. The selection of the different topographies was based on the water-repellent effect of the leaves of these plants. The hydrophobic behavior can be explained by a micro- and nanoscopic design of the topography of the leaves[13]. The double structure consists of papillae epidermal cells and an additional layer of epicuticular waxes. The surface pattern of the leaves was studied using a SEM and a 3D-profilometer in order to determine the structures. SEM images of the Oryzasativa's double structure of the leaves are shown in Fig. 1 as examples of the leave structure of this plant.

Developing bionic structures, it is essential to consider manufacturing aspects related to the geometry since its complexity is limited by the structuring technique. An appropriate method to manufacture highly accurate bionic structures on tool steels is micromilling[14]. For this, the geometry of the structures was adjusted to the shape of the cutting edge of the milling tools. The developed bionic structures are schematically illustrated in Fig. 2. Structure St1 is based on the bamboo plant Sasapalmata and consists of rectangular inner curvatures with a length of 360 μm, a width of 260 μm, and a depth of 10 μm. The Phyllostachys bamboo plant is used as a source of inspiration for structure St2. This structure is characterized by two straight v-shaped grooves with a width of 10 μm and a depth of 10 μm each, with a distance of 30 μm between the individual grooves. Structure St3 is based on Euphorbia myrsinites and consists of circular with 10 μm bumps, which flatten tangentially to the ground area. A single bump is surrounded by six other bumps within a range of 110 μm. Structure St4 is inspired by the bamboo plant Chusqueaspectabilis and consists of straight, semicircular grooves with a width of 110 μm and a depth of 20 μm, which are arranged 30 μm apart from each other. The rice plant Oryza sativa inspired structure St5, which has a wave-like structure with a depth of 20 μm and cyclic bumps at a distance of 200 μm.

Except the bumps of structure St3, each structure is characterized by an anisotropic pattern. The directional dependency is illustrated with *x*- and *y*-coordinates in Fig. 3.

Micromilling is a filigree advanced machining process and it is the only technique that enables to

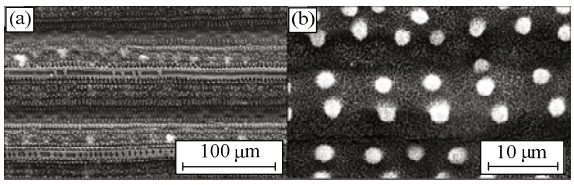

Fig. 1 SEM images of the (a) microscopic and (b) nanoscopic structure of Oryza sativaleaves.

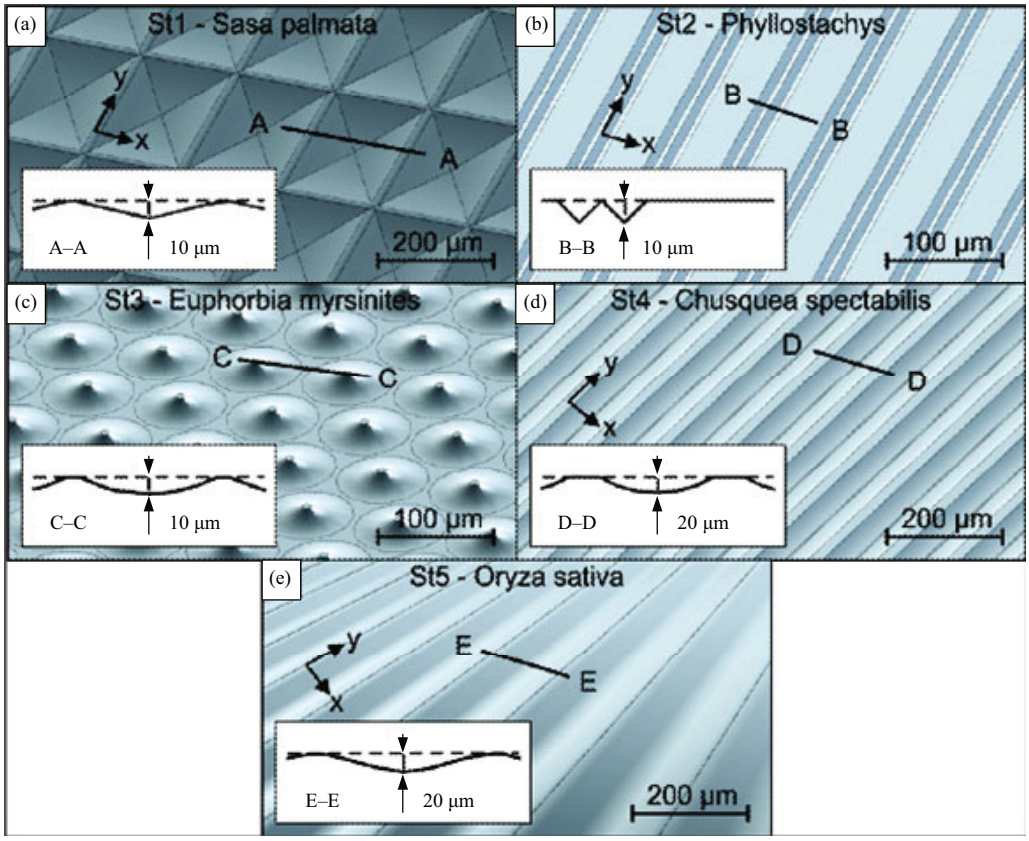

Fig. 2 Schematics of the developed bionic structures. (a) Sasapalmata; (b) Phyllostachys; (c) Euphorbia myrsinites; (d) Chusqueaspectabilis; (e) Oryziasativa.

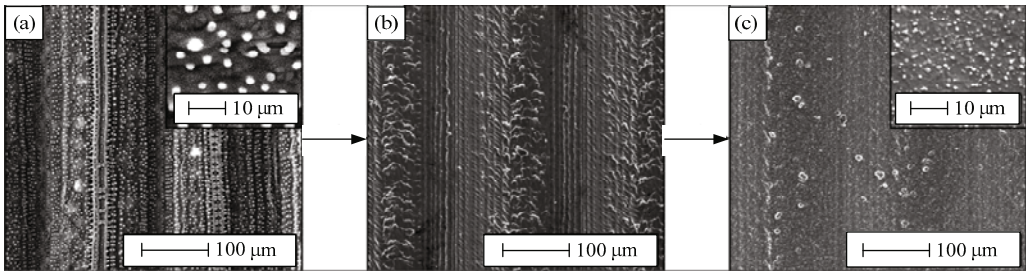

Fig. 3 Process steps to replicate the (a) micro- and nanostructure of plants on steel by (b) micromilling and (c) plasma-nitriding.

reproduce the microscopic structure of the leaves. One approach to generate a nanostructure is the plasma-nitriding process. Plasma-nitriding does not only increase the surface hardness but also leads to a needle-shaped formation of the iron nitride Fe4N with a diameter of a few nanometers on the surface[15]. Thereby, bionic structures obtain an additional nanoscopic structure and form a double structure, which is similar to the surface of hydrophobic plants. Therefore, nitride needles are formed on purpose in order to generate both a nano- and a macroscopic structure. The process of replicating the micro- and nanostructure of the plants on steel is shown in Fig. 3.

2.2 Heat-treatment and surface modifications

The chosen modifications included four main steps: heat treatment, surface structuring, plasma-nitriding, and PVD deposition. After each process, the influence of the modification on the resulting topography as well as the wetting behavior is analyzed and discussed in the next section.

The powder metallurgically manufactured high-speed steel ASP® 2023 was selected for the investigations. Besides the as-delivered annealed condition, the

samples underwent a heat treatment, consisting of hardening at 1100 ˚C and tempering at 560 ˚C for three times. Detailed information concerning the hardness depth profiles as well as the residual stresses in the subsurface area and the PVD-coating adhesion due to different heat and plasma-treatments can be found in previous studies by the authors[16,17].

The ASP® 2023 steel was structured by means of micromilling, using the HSPC 2522 (Kern Microtechnik, Germany) machine at the Institute of Machining Technology. Different types of cutting tools consisting of ultra-finely-grained cemented carbides were used in order to process the bionic structures, as shown in Fig. 4. The detailed information about the used tools as well as the structuring time of the corresponding bionic structures are summarized in Table 1.

The plasma-nitriding process was realized within an Arc-PVD device PVD20 (Metaplas, Germany). The samples were plasma-nitrided in a H2-N2-atmosphere with a volumetric ratio of 3:1 at a temperature of 560 ˚C for 8 hours as reported in previous studies[16,17]. The inhibition of nitrogen diffusion further affects the formation of iron nitride Fe4N on the surface of the steel as the annealed-nitrided steel exhibits a higher amount of needle-shaped nitrides on the surface (see Fig. 5).

An industrial magnetron sputtering device CC800/9 Custom (CemeCon AG, Germany) was used to deposit the CrAlN coatings. More details about the deposition process of the CrAlN coating can be found in Ref. [18]. The deposition time was adapted for the depositions to obtain a coating thickness of 2.5 µm. All substrates were treated differently and coated with CrAlN thin films, showing the same morphology and mechanical properties. The deposited CrAlN thin films have a chemical composition of 13.8 ± 0.2 at.-% Cr, 35.3 ± 0.6 at.-% Al, and 51.0 ± 0.8 at.-% N. The coatings are characterized by a fully-dense microstructure with a hardness of 22.06 GPa ± 2.47 GPa and a Young's modulus of 355.9 GPa ± 37.1 GPa. Fig. 6 shows SEM images of the morphology of the CrAlN coatings.

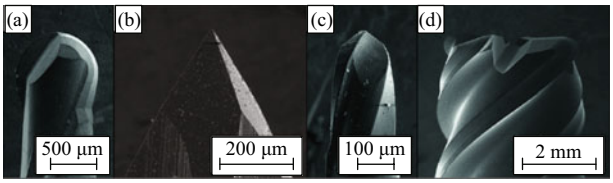

Fig. 4 SEM images of (a) a ball cutter with a diameter of 1 mm, (b) a deburring tool, (c) a ball cutter with a diameter of 0.2 mm, and (d) a torus cutter with a diameter of 4 mm.

Table 1 Overview of the used cutter tools and the structuring time for each structure

Surface structure	Cutter type	Tool geometry	Structuring time ($mm^2 \cdot min^{-1}$)
Plain-milled	Torus cutter	Ø = 4 mm	53.00
St1	Ball cutter	Ø = 1 mm	6.40
St2	Deburrer	90˚ cutting edge	6.40
St3	Ball cutter	Ø = 0.2 mm	0.34
St4	Ball cutter	Ø = 0.2 mm	3.20
St5	Ball cutter	Ø = 0.2 mm	4.92

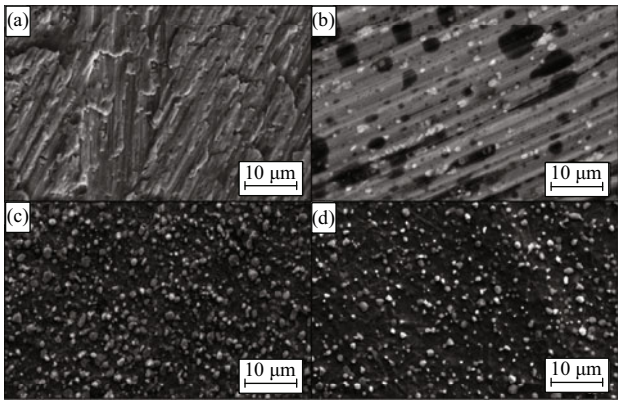

Fig. 5 SEM images of the topography of (a) annealed, (b) tempered, (c) annealed-nitrided, and (d) tempered-nitrided ASP® 2023.

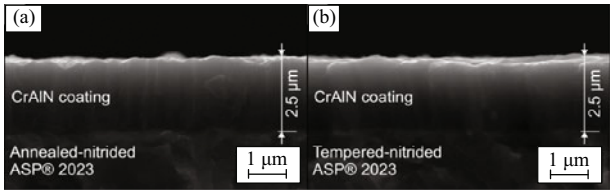

Fig. 6 CrAlN coatings on (a) annealed-nitrided and (b) tempered-nitrided ASP® 2023.

2.3 Measuring and analyzing techniques

The surface analyses of the bionic structures and the reference samples were carried out by means of a 3D profilometer and SEM. The 3D profilometer InfiniteFocus (Alicona, Austria) was used to measure the geometry of the structures. Subsequently, the 3D images were examined with the aid of the software µsoft Analysis Premium 5.1 at the Institute of Machining Technology. In addition, the surface topography of the samples was analyzed utilizing the Field Emission Scanning Electron Microscope FE-JSEM 7001 (Jeol, Japan).

The wettability of the bionic structures and the plain-milled reference surface were analyzed by the contact angle measuring system G40 (Krüss, Germany). The differently modified surfaces were wetted with distilled water and a deep drawing oil (Berufluid ST6007 (Carl Bechem GmbH, Germany)) using a volume of 5 µl of each fluid. This mineral oil-free forming lubricant (viscosity $\eta = 160\ mm^2 \cdot s^{-1}$ at 20 ˚C) is used to form steel sheets of up to 4 mm and thus perfectly meets the needs of SBMF processes. As the anisotropy of the structures has an influence on the wetting behavior[19], the wetting tests were carried out in x and y-direction for each structure and treated surface. All measurements were conducted at room temperature and 10 repetitions were performed for each test.

3 Results and discussion

3.1 Influence of the process steps on the structural geometry

For the subsequent investigation of the wetting behavior, it is necessary to analyze the geometry and topography of the bionic structures in order to evaluate the influence of the treatment on the wettability. For this reason, the structural geometry and surface topography were analyzed after each process step.

3.1.1 Structure geometry and surface topography after micromilling

The micromilled structures were analyzed concerning their geometry and topography. 3D images and roughness values of the bionic structures after the micromilling process are presented in Fig. 7. On the left side of the respective images, the high-speed steel ASP® 2023 is shown in annealed condition, while the right side shows its hardened and tempered condition. Structure St1 features the rectangular inner curvatures with a depth of 10 µm and fulfills the geometric specification. Structure St2 strongly deviates from the desired geometry, as it does not consist of v-shaped grooves but rather of closely packed furrows. The resulting geometry emerges from the dynamic wear behavior of the used deburrer tool, the 90˚ cutting edge of which wore out during the machining process. However, structure St2 exhibits a reproducible geometry and was therefore used in the subsequent studies. The milled structure St3 features the demanded shape of circular bumps but presents a slight depth deviation of 2 µm. The structures St4 and St5 also have the demanded geometry, but demonstrate a minor depth deviation. The small deviation of these structures is caused by a manufacturing tolerance of the micromilling machine and the tool wear. However, most of these bionic structures feature an almost identical geometry compared to the plants with a high accuracy.

Besides the shape, the surfaces of the structure are distinguished by different topographies. The roughness of the structures is influenced by the heat treatment of the high-speed steel. Micromilled steel in annealed condition has a higher roughness than tempered steel. For instance, structure St1, annealed steel, is characterized by a mean roughness depth R_z of 7.58 µm ± 0.18 µm in x-direction and 4.25 µm ± 0.06 µm in y-direction, while the tempered counterpart exhibits lower values of 6.12 µm ± 0.36 µm in x-direction and 3.16µm ± 0.06 µm in y-direction. A close investigation of the topography is conducted by SEM analyses. SEM images of structure St1 with both steel conditions are exemplary shown in Fig. 8. The structured surface on the annealed steel has a rough and uneven topography with micro burrs, while the structure on tempered steel has a smoother surface with less micro burrs. The different topographies can be explained by the microstructure of the heat treated high-speed steel since the type and size of the grains have an influence on the roughness of micro-machined surfaces[20]. The annealed microstructure consists of ferrite with a high ductility, while the hardened and tempered steel has a martensitic structure[21]. The martensitic structure is characterized by a higher deformability than ferrite and thus ensures a higher geometrical accuracy and surface quality when being machined. Furthermore, multi-phase ductile steel exhibits a higher roughness than single-phase steel as the cutting process is interrupted at the grain boundaries, thus causing micro burrs[22].

3.1.2 Structure geometry and surface topography after plasma-nitriding and PVD-deposition

The bionic structures were analyzed after being plasma-nitrided and coated with a CrAlN thin film in order to evaluate a possible influence of the treatments on the geometry and topography. The treatments do not lead to an alteration of the shape as the bionic structures maintain their geometry due to the near-net shape PVD-coating. This is exemplary visible in the false color images for structure St5 with annealed as well as hardened and tempered steel in Fig. 9. However, an

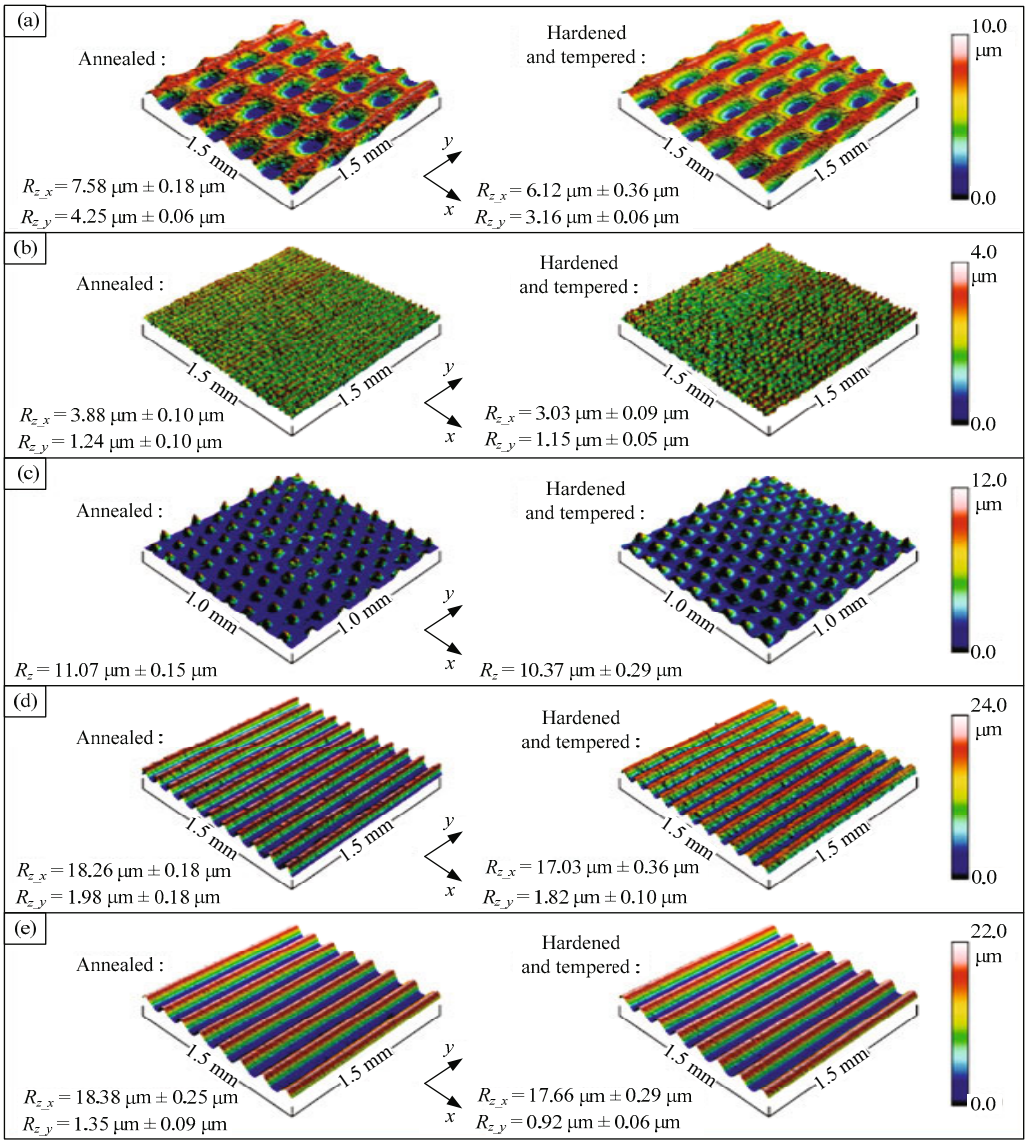

Fig. 7 3D images and roughness values of (a) St1, (b) St2, (c) St3, (d) St4, and (e) St5 structured on annealed, hardened, and tempered ASP® 2023.

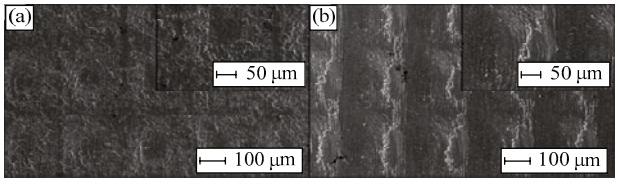

Fig. 8 SEM images of St1 structured on (a) annealed and (b) hardened and tempered ASP® 2023.

increase of the roughness is recognizable after each treatment. The mean roughness depth R_z of structure St5 with annealed steel increases from 13.38 µm ± 0.25 µm in *x*-direction and 1.35 µm ± 0.09 µm in *y*-direction to 18.54 µm ± 0.25 µm and 1.50 µm ± 0.15 µm. The increase of the roughness of nitrided structures can be explained with the formation of Fe4N nitriding needles on the surface. In addition, the deposition of the CrAlN thin film leads to a further increase of the roughness. The R_z values of the coated structure St5, annealed-nitrided steel, increase to 19.47 µm ± 0.22 µm in *x*-direction and 2.26 µm ±0.16 µm in *y*-direction. In this case, the rise is caused by the cauliflower like topography of the CrAlN thin films.

3.2 Wetting behavior of bionic structures

The measured contact angles of the bionic structures in each process state when wetted with distilled water as well as with deep drawing oil Berufluid ST 6007 are given in Figs. 10–15. The bar chart on the left

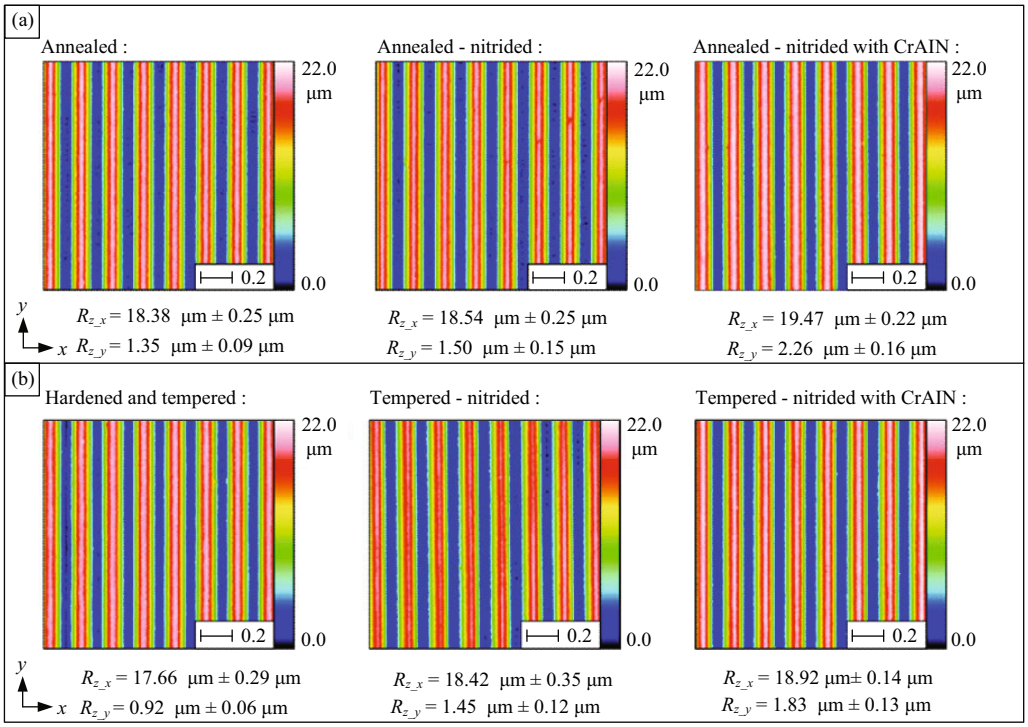

Fig. 9 3D images and roughness values of St5 after each process treatment with (a) annealed and (b) hardened and tempered ASP® 2023.

shows the contact angle values in *x*-direction of the structures, while the values in *y*-direction are given on the right.

3.2.1 Wetting behavior after micromilling

The contact angles of micromilled steel in annealed as well as hardened and tempered condition are shown in Figs. 10 and 11. All structured surfaces possess larger contact angles than the plain-milled surface when wetted with a drop of water. This wetting behavior is observed for all structures after each process step. Furthermore, the shape of the water drop is not spherical as it is strongly influenced by the directional dependency of the structures St1, St2, St4, and St5. For instance, structure St2, annealed steel, exhibits contact angles of 84.1° ± 2.0° in *x*-direction and 68.6° ± 1.3° in *y*-direction. The *y*-direction of these structures is characterized by the orientation of the grooves while the elavations are perpendicular to them. All anisotropic structures exhibit larger contact angles in *x*-direction than that in *y*-direction. In addition, the contact angles in both directions are higher than the value of the plain-milled surfaces. This wetting behavior can be explained with the observation of Chen *et al*. who investigated the wetting of anisotropic rough surfaces[19]. They noticed that a water drop is trapped in a state where it resides on pillars of parallel grooves. The contact angles of the drop are different and both larger than the intrinsic value of the substrate material. The pillars act as local energy barriers and hence separate the water drop from neighboring lower energy states of the surface. These energy barriers prevent the spreading of the water drop in *x*-direction. As a result, the contact angle in *x*-direction is larger than that in *y*-direction. Furthermore, structures St2 and St4 tend to have the largest angles in *x*-direction for each process state of the sample. Comparing the structural geometry, it becomes evident that both bionic structures are characterized by a greater number of bumps in *x*-direction. Therefore, the spreading of the water drop is stopped by more energy barriers and the water is not able to wet the surface with smaller angles. However, compared to St2 or St4, structure St1 does not feature as many elevations and the spreading of the water drop is not hindered by many energy barriers. Thus, St1 has smaller contact angles than the other anisotropic structures. As structure St3 has an isotropic structural geometry, the water drop spreads uniformly in both directions and has a spherical shape. Structure St3 with annealed as well as hardened and tempered steel is characterized by contact angles of 79.6° ± 2.2° and 80.1° ± 1.5°, respectively. In addition to

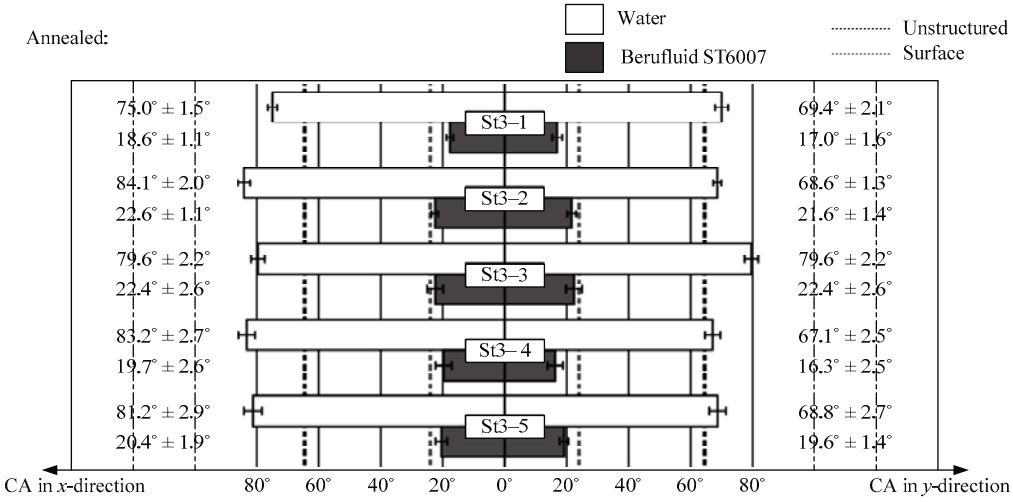

Fig. 10 Contact angles of bionic structures with annealed steel.

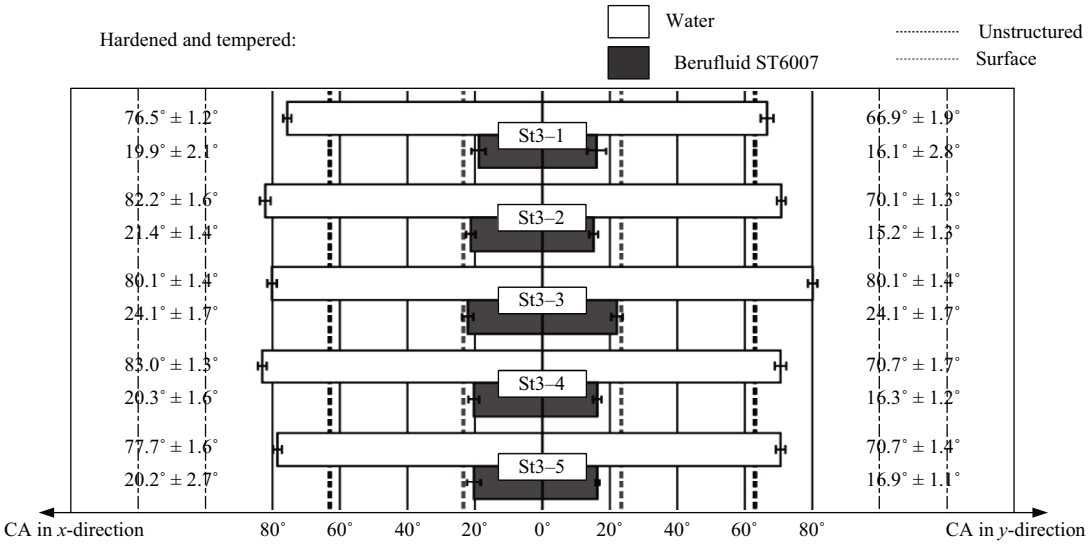

Fig. 11 Contact angles of bionic structures with hardened and tempered steel.

the water drop, the structural cavaties of all bionic structures were wetted with a thin water film. The co-existence of a drop and a film was already observed by Bico *et al*. and defined as a "composite drop"[23]. In case of structured surfaces of a hydrophilic material, the water drop spreads inside the solid cavaties and coexists with the solid filled liquid film. Between the two heat treatments of the high-speed steel, no significant difference concerning the wetting behavior could be observed. Annealed as well as hardened and tempered structures exhibit contact angles values in an equal dimension.

When wetted with Berufluid ST 6007, the surfaces present lower contact angle values than that surfaces wetted with a water drop. This behavior is related to the high viscosity of the forming lubricant. The annealed plain-milled surfaces as well as hardened and tempered steel show the values of 24.0° ± 1.8° and 23.3° ± 2.3°, respectively. Except structure St3, the structured surfaces exhibit lower values ranging from 15.2° to 22.6° than the unstructured counterparts. Due to the high viscosity, the lubricant spreads into the structural cavities and, by wetting these areas, leads to small contact angles. However, this behavior is not observed for structure St3 as its bumps block the spreading of the lubricant. A directional dependency of the wetting behavior is further observed for the anisotropic structures St1, St2, St4, and St5. Similar to the wetting with a water drop, the structures are characterized by a larger contact angle value in *x*-direction than that in *y*-direction.

3.2.2 Wetting behavior after plasma-nitriding

The measurement results of the contact angles for the bionic structures after plasma-nitriding are listed in Figs. 12–13. The plasma-nitrided structures possess larger contact angle values than the unstructured surfaces when wetted with a water droplet. The plain-milled steel with annealed as well as hardened and tempered steel have the contact angles of 64.7˚ ± 1.6˚ and 63.9˚ ± 1.7˚ after being plasma-nitrided. The bionic structures in annealed-nitrided condition show the values between 66.6˚ and 87.6˚, while the tempered-nitrided counterpart shows the contact angles ranging from 70.4˚ to 83.1˚. The wide range of values of the annealed-nitrided structures can be explained by outlier values since most of the contact angles are within the same range as of the tempered-nitrided variant. Since plasma-nitriding does not affect the shape of the structured surfaces, the anisotropic structures St1, St2, St4, and St5 still show a direction dependent wetting behavior. The wetting of plasma-nitrided surfaces with Berufluid ST 6007 shows a similar behavior for the untreated structures. The structures have smaller contact angle values than the unstructured surfaces. However, the plasma-nitrided surfaces do not show any significant change in the wetting behavior. Even though the plasma-nitriding process generated a nanoscopic structure on the surface, no substantial influence on the wetting could be observed. This is due to the randomly distributed nitriding needles, which do not follow a required deterministic pattern. In addition, the diffusion of nitrogen into the surface layer should cause a change of the surface energy, thus influencing the wetting behavior. Tang *et al*. proved in their work that a plasma treatment increases the surface energy of stainless steel[24]. However, such a correlation was not observed after plasma-nitriding the structured surfaces. Furthermore, the plasma-nitriding process causes an increase of the roughness, as discussed in section **3.1.2**. According to Wenzel's theory, the surface roughness enhances the wettability[25]. Therefore, the combination of plasma-nitriding and the increase in resulting roughness should induce a change of the contact angle due to the effect of nanoscale surface modifications. However, the structured surfaces are characterized by macroscopic dimensions, which seem to superimpose the nanoscopic effects. Therefore, the wetting behavior remains on an equal level.

3.2.3 Wetting behavior after PVD-deposition

The measured contact angles of the structured surfaces after the PVD-deposition are given in Figs. 14–15. When wetted with water, the coated structures have larger contact angles than the unstructured surfaces. Unstructured surfaces with annealed-nitrided and tempered-nitrided steel have the contact angles of 62.2˚ ± 2.3˚ and 62.8˚ ± 2.1˚ after the deposition. The CrAlN coated structures have the contact angles between 68.1˚ and 82.0˚. Furthermore, the direction dependent wetting behavior applies to the anisotropic structures as well. As described in sections **3.1.1** and **3.1.2**, the larger contact angles with the water drop are formed due to the structural elevations that act as energy barriers.

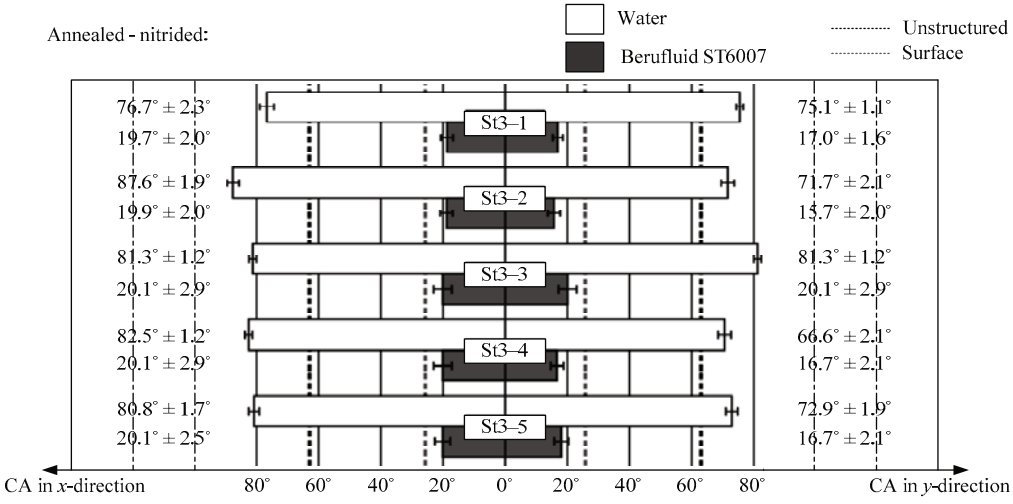

Fig. 12 Contact angles of bionic structures with annealed-nitrided steel.

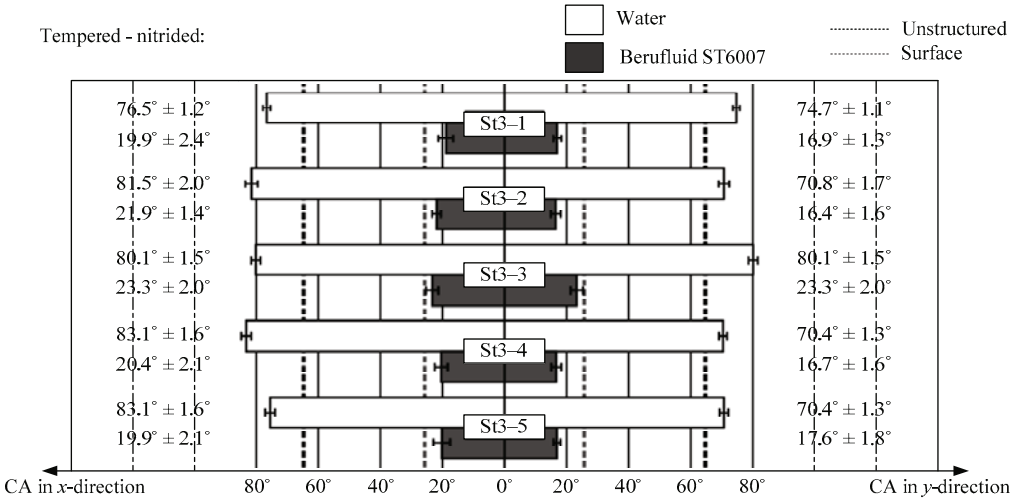

Fig. 13 Contact angles of bionic structures with tempered-nitrided steel.

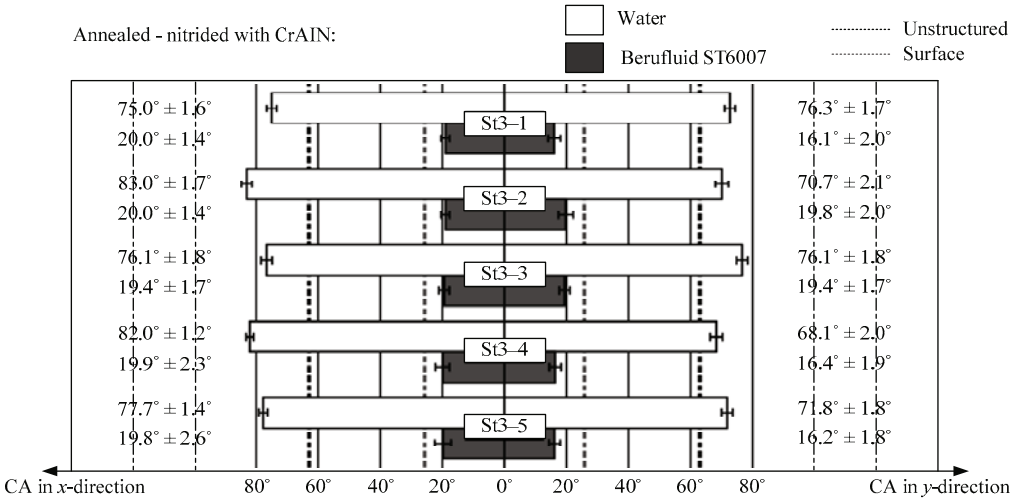

Fig. 14 Contact angles of bionic structures with annealed-nitrided steel and CrAlN coating.

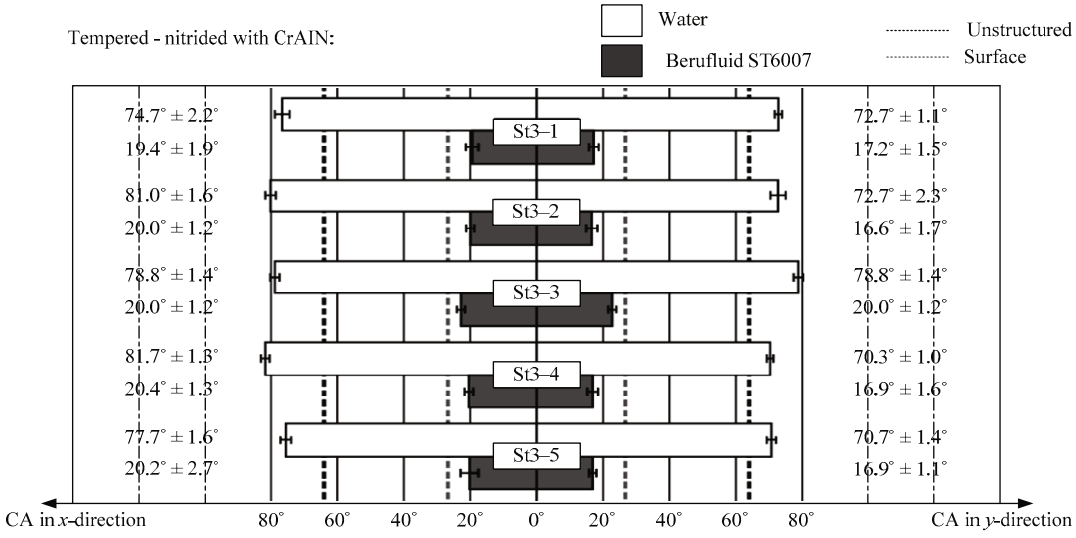

Fig. 15 Contact angles of bionic structures with tempered-nitrided steel and CrAlN coating.

The CrAlN coated structures present the same tendencies as the uncoated structures when wetted with Berufluid ST 6007. The bionic structures also exhibit smaller contact angles than the unstructured surfaces. The structures have the contact angles ranging from 16.1˚ to 20.4˚, while the unstructured surfaces with annealed-nitrided and tempered-nitrided steel exhibit angles of 22.0˚ ± 1.7˚ and 22.3˚ ± 1.1˚, respectively. In addition, the anisotropic wetting behavior with the lubricant is observed for structures St1, St2, St4, and St5.

According to the current state of knowledge, Cr-based thin films have a low surface energy and thus larger contact angles than steel wetted with water[26]. Within our investigations, a difference between CrAlN coated and uncoated structures was not detected, as the structures exhibit similar contact angles after deposition. The increase in roughness can be considered to be a possible cause for this behavior. Besides the influence of the surface energy, the wetting with fluids is also affected by the surface roughness.

4 Summary and outlook

Bionic structures, based on models from the flora were developed and successfully applied onto high-speed steel for SBMF tools. The heat-treatment affects the surface topography of the micromilled surfaces since the micromilling process is influenced by the microstructure of the steel. Further treatments consisting of plasma-nitriding and PVD-deposition lead to an increase of the roughness due to the formation of nitride needles and growth defects of the CrAlN thin film. However, the treatments do not have an impact on the shape of the structures.

The wetting behavior with fluids can be influenced by structuring surfaces. The bionic structures exhibit higher contact angles than the unstructured surfaces when wetted with a water droplet. The anisotropy of the structures influences the wetting with water, as the structural elevations act as energy barriers and block the spreading of water. Thereby, higher contact angle values are achieved when the surfaces are wetted with water. A contrary behavior is observed for the deep drawing oil Berufluid ST 6007. Due to its higher viscosity compared to water, the lubricant spreads easier into the structural cavities. Thereby, the structured surfaces feature smaller contact angles than plain-milled surfaces when wetted with a forming lubricant. Therefore, structuring tool surfaces is a method to locally adjust the wettability with lubricants, thus changing the friction condition with a counterpart. Further tribological investigations need to be conducted in order to evaluate the influence of the wetting behavior during real forming processes. One of the major aspects for further research is to adjust the topography of PVD thin films by changing the bias voltage.

Acknowledgment

This work was supported by the German Research Foundation (DFG) within the Transregional Collaborative Research Centre CRC/TR 73 subproject B5. Furthermore, the authors thank Prof. Dr.-Ing. Dirk Biermann and Dipl.-Ing. Eugen Krebs of the Institute of Machining Technology (TU Dortmund) for manufacturing the bionic structures as well as Dr. rer. nat. Frank Katzenberg and Prof. Dr. rer. nat. Jörg C. Tiller of the Biomaterials and Polymer Science Department (TU Dortmund) for providing the contact angle measuring system. Furthermore, the authors wish to express their gratitude to Carl Bechem for providing lubricants for the experiments. The authors are further grateful to Andreas Fischbach of the Botanical Garden at the HeinrichHeine University Düsseldorf and Annette J. Höggemeier of the Botanical Garden at the Ruhr University Bochum for providing the plants.

References

[1] Merklein M, Koch J, Schneider T, Opel S, Vierzigmann U. Manufacturing of complex functional components with variants by using a new metal forming process–sheet-bulk metal forming. *International Journal of Material Forming*, 2010, **3**, 347–350.

[2] Merklein M, Allwood J M, Behrens B A, Brosius A, Hagenah H, Kuzman K, Mori K, Tekkaya A E, Weckenmanng A. Bulk forming of sheet metal. *CIRP Annals-Manufacturing Technology*, 2012, **61**, 725–745.

[3] Subramonian S, Kardes N. Materials for sheet forming. In Altan E, Tekkaya A E (eds.), *Sheet Metal Forming*: *Fundamentals*, 1st ed, ASM International, Ohio, USA, 2012, 73–88.

[4] Kersting P, Gröbel D, Merklein M, Sieczkarek P, Wernicke S, Tekkaya A, Krebs E, Freiburg D, Biermann D, Weikert T, Tremmel S, Stangier D, Tillmann W, Matthias S, Reithmeier E, Löffler M, Beyer F, Willner K. Experimental and numcerial analysis of tribological effective surfaces for forming

tools in sheet-bulk metal forming. *Production Engineering*, 2016, **10**, 37–50.

[5] Tillmann W, Dildrop M, Sprute T. Influence of nitriding parameters on the tribological properties and the adhesion of Ti- and Cr-based multilayer designs. *Surface and Coatings Technology*, 2014, **260**, 380–385.

[6] Merklein M, Schrader T, Engel U. Wear behavior of PVD-coatings. *Tribology in Industry*, 2012, **34**, 51–56.

[7] Vetter J, Knaup R, Dweletzki H, Schneider E, Vogler S. Hard coatings for lubrication reduction in metal forming. *Surface and Coatings Technology*, 1996, **86**–**87**, 739–747.

[8] Hetzner H, Koch J, Tremmel S, Wartzack S, Merklein M. Improved sheet bulk metal forming processes by local adjustment of tribological properties. *Journal of Manufacturing Science and Engineering*, 2011, **133**, 061011.

[9] Tillmann W, Vogli E, Herper J, Haase M. Nanostructured bionic PVD-coatings for forming tools. *Key Engineering Materials*, 2010, **438**, 41–48.

[10] Tillmann W, Herper J, Laemmerhirt I A. Development and tribological investigation of the coating system Chromium Carbonitride (CrCN) to different surface designs. *Journal of Materials Science and Engineering B* 2, 2012, **4**, 223–229.

[11] Herper J. *Tribologische Untersuchungen von Verschleiß- und Reibungsarmen Nanostrukturierten Bionischen PVD-Beschichtungen*. 1st ed, Vulkan-Verlag, Essen, Germany, 2013. (in German)

[12] Guan H Y, Han Z W, Cao H N, Niu S C, Qian Z H, Ye J F, Ren L Q. Characterization of multi-scale morphology and superhydrophobicity of water bamboo leaves and biomimetic polydimethylsiloxane (PDMS) replicas. *Journal of Bionic Engineering*, 2015, **12**, 624–633.

[13] Barthlott W, Neinhuis C. Purity of the sacred lotus, or escape from contamination in biological surfaces. *Planta*, 1997, **202**, 1–8.

[14] Biermann D, Krebs E, Schlenker J. Micromilling of bionic structures. *Proceedings ASPE* 2011 *Spring Topical Meeting – Structured and Freeform Surfaces*, Charlotte, USA, 2011, 120–125.

[15] Gontijo L C, Machado R, Miola E J, Casteletti LC, Nascente P A P. Characterization of plasma-nitrided iron by XRD, SEM and XPS. *Surface and Coatings Technology*, 2004, **183**, 10–17.

[16] Denkena B, Grove T, Lucas H, Tillmann W, Stangier D. Influence of PVD-coating manufacturing steps on the subsurface integrity of hardened and soft AISI M3:2 high speed steel. In Bobzin K, Bouzakis K D, Denkena B, Maier H J, Merklein M (eds.), *Proceedings of the* 12*th International Conference THE* "*A*" *Coatings*, PZH Verlag, Germany, 2016, 23–30.

[17] Tillmann W, Stangier D, Denkena B, Grove T, Lucas H. Influence of PVD-coating technology and pretreatments on residual stresses for sheet-bulk metal forming tools. *Productions Engineering*, 2016, **10**, 17–24.

[18] Tillmann W, Stangier D, Laemmerhirt I-A, Biermann D, Freiburg D. Investigation of the tribological properties of high-feed-milled structures and Cr-based hard PVD-coatings. *Vacuum*, 2016, **131**, 5–13.

[19] Chen Y, He B, Lee J, Patankar N A. Anisotropy in the wetting of rough surfaces. *Journal of Colloid and Interface Science*, 2005, **281**, 458–464.

[20] Pham D T, Dimov S S, Popov K B, Elkaseer A M A. Effects of microstructure on surface roughness and burr formation in micromilling: A review. *Proceedings of the* 4th *Virtual International Conference on Innovative Production Machines and Systems* (*IPROMS*), Cardiff, United Kingdom, 2008, 270–257.

[21] Bayer A M, Becherer B A, Vasco T. *High-speed Tool Steels*. ASM Handbook, ASM International, USA, 1989, **16**, 51–59.

[22] Vogler M P, DeVor R E, Kapoor S G. On the modeling and analysis of machining performance in micro-endmilling, part I: Surface generation. *Journal of Manufacturing Science and Engineering*, 2004, **126**, 685–694.

[23] Bico J, Thiele U, Quéré D. Wetting of textured surfaces. *Colloids and Surfaces A*: *Physicochemical and Engineering Aspects*, 2002, **206**, 41–46.

[24] Tang S, Kwon, O, Lu N, Choi H. Surface characteristics of AISI 304L stainless steel after an atmospheric pressure plasma treatment. *Surface and Coatings Technology*, 2005, **195**, 298–306.

[25] Wenzel R. Resistance of solid surfaces to wetting by water. *Industrial and Engineering Chemistry*, 1936, **28**, 988–994.

[26] Lugscheider E, Bobzin K. The influence on surface free energy of PVD-coatings. *Surface and Coatings Technology*, 2001, **142**–**144**, 755–760.